ISSN 1070-3284, Russian Journal of Coordination Chemistry, 2022, Vol. 48, No. 8, pp. 464–477. © Pleiades Publishing, Ltd., 2022.
Russian Text © The Author(s), 2022, published in Koordinatsionnaya Khimiya, 2022, Vol. 48, No. 8, pp. 458–472.

The issue is dedicated to the 70th birthday of Academician V.I. Ovcharenko

Redox-Active Germylene Based on 2,4,6,8-Tetra-*tert*-butylphenoxazin-1-one: Synthesis, Structure, and Chemical Properties

K. V. Arsenyeva[a], A. V. Klimashevskaya[a], M. A. Zherebtsov[a], M. G. Chegerev[b], A. V. Cherkasov[a], I. A. Yakushev[c], and A. V. Piskunov[a, *]

[a] *Razuvaev Institute of Organometallic Chemistry, Russian Academy of Sciences, Nizhny Novgorod, Russia*
[b] *Research Institute of Physical and Organic Chemistry, Southern Federal University, Rostov-on-Don, Russia*
[c] *Kurnakov Institute of General and Inorganic Chemistry, Russian Academy of Sciences, Moscow, Russia*
**e-mail: pial@iomc.ras.ru*

Received December 2, 2021; revised December 20, 2021; accepted December 24, 2021

Abstract—New complex of low-valent germanium ^{Phenox}APGe (**I**) based on the redox-active ligand 2,4,6,8-tetra-*tert*-butylphenoxazin-1-one is synthesized and structurally characterized. Its versatile reactivity is demonstrated for the acid-base and redox transformations. The reaction of germylene **I** with $Ni(COD)_2$ is found to result in the substitution of both cyclooctadiene molecules, coordination of four germylene fragments to zero-valent nickel, and formation of compound $(^{Phenox}APGe)_4Ni$ (**II**). The reaction of compound **I** with $[CpNi(CO)]_2$ in a toluene solution affords complex $(^{Phenox}APGe)_2(NiCp)_2$ (**III**), being the substitution product of two carbonyl groups by two isolobal germylene fragments. The reaction with the one-electron oxidant (3,6-di-*tert*-butyl-2-methoxyphenoxyl radical) generates labile paramagnetic germylene **IV** characterized by EPR spectroscopy. Digermylene oxide **V** synthesized by the hydrolysis of the starting germylene **I** *in situ* reacts with *N*-heterocyclic carbene and KC_8 to form ionic derivatives **VI** and **VII** containing the Ge(II)–O–Ge(II) fragment. Germylene **I** is tested as a catalyst for the hydroboration of benzaldehyde. The molecular structures of the compounds are determined by X-ray diffraction (CIF files CCDC nos. 2117783 (**I**), 2124277 (**II**), 2125357 (**III**), and 2118393 (**VII**)).

Keywords: germanium, carbene analogs, one-electron oxidation, X-ray diffraction, EPR, hydroboration

DOI: 10.1134/S1070328422070016

INTRODUCTION

The vigorous development of the trend related to low-valent derivatives of nontransition metals is observed in the recent decade in coordination and organoelement chemistry [1–3]. Although these studies are primarily fundamental, compounds of this type demonstrate a promising reactivity toward the activation of small molecules [4–6]. This provides prospects of using the compounds of nontransition elements in low oxidation states in catalytic processes. The search for nonmetallic catalysts is continued in terms of this concept. Increasing interest in processes with a lower environmental effect stimulates the search for improved synthetic transformations with the minimum formation of waste and a lower power consumption and excluding the formation of toxic substances. One of the approaches to achieving this purpose is the use of more safe compounds of the main group as catalysts [7].

The systems based on α-diimines are actively applied for the stabilization of low-valent states of groups 12, 13, and 14 [8–10] elements. Among a large variety of ligands of diverse nature, there are examples of successful using the closest analogs of diimines (*o*-iminoquinones (imQ)) as systems capable of stabilize nontransition metals in low oxidation states [11–16].

o-Iminoquinones are striking representatives of redox-active organic ligands. The compounds containing ligands of this type are being studied intensively [17–20], possess unique magnetic and electronic properties [21–25], and find use as spin labels [26]. Their EPR spectra are highly informative and can provide diverse data on the structures and mechanisms of the transformations [26–30].

2,4,6,8-Tetra-*tert*-butylphenoxazin-1-one is an interesting example of a redox-active ligand [31]. In spite of the fact that this compound has been synthesized rather long ago, the number of compounds based on this tricyclic iminoquinone is restricted by a few complexes in which the ligand exists in the dianionic [32] or anion-radical states [33–39]. The first studies in the area of the coordination chemistry of 2,4,6,8-tetra-*tert*-butylphenoxazin-1-one were carried out in the framework of studying the paramagnetic derivatives of various metals in solutions by EPR spectroscopy [31]. The range of metals was enlarged much later. There are completely characterized compounds of the metals of groups 8 [39–41], 9 [34, 42], 10 [39], 11 [43], 12 [36], and 14 [32, 35].

Scientific interests of our research group lie in the area of studying heavy *O*,*N*-heterocyclic analogs of carbenes based on the sterically hindered *o*-amidophenolate ligands. Earlier we successfully studied diverse chemical properties of the compounds of group 14 elements in low oxidation states: oxidative addition proceeding at the metal or ligand, reduction of the metal center, acid-base interactions, and catalytic activity [11–16, 44, 45]. In this study, we used 2,4,6,8-tetra-*tert*-butylphenoxazin-1-one for the stabilization of the low-valent state of germanium and studied the chemical behavior of the synthesized complex.

EXPERIMENTAL

All procedures on the synthesis and study of chemical transformations of the germanium complexes were carried out without air oxygen and moisture. The solvents used were purified and dehydrated according to published recommendations [46]. Commercial reagents $GeCl_2$·diox and $Ni(COD)_2$ were used. 2,4,6,8-Tetra-*tert*-butylphenoxazin-1-one [32] and 1,3-diisopropyl-4,5-dimethylimidazol-2-ylidene [47] were synthesized according to known procedures.

NMR spectra were recorded on Bruker Avance Neo 300 MHz and Bruker 200 MHz spectrometers. EPR spectra were detected on a Bruker EMX spectrometer. 2,2-Diphenyl-1-picrylhydrazyl ($g = 2.0037$) served as the standard for the determination of the *g* factor. To determine precise parameters, the EPR spectrum was simulated using the WinEPR SimFonia program (Bruker). Elemental analysis was carried out on an Elementar Vario El cube instrument.

Synthesis of 3,6-di-*tert*-butyl-4-(3,6-di-*tert*-butyl-2-methoxyphenoxy)-2-methoxycyclohexa-2,5-dien-1-one that reversibly dissociates to form two 2-methoxy-3,6-di-*tert*-butylphenoxy radicals was carried out using an earlier published approach [48].

3,6-Di-tert-butyl-2-methoxyphenol.

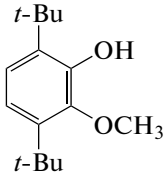

3,6-Di-*tert*-butylpyrocatechol (9.75 g, 0.044 mol) was dissolved in *N*,*N*-dimethylformamide (100 mL), and iodomethane (6.25 g, 0.044 mol) and then potassium carbonate (6.07 g, 0.044 mol) were added. The reaction mixture was held at 60°C for 24 h. After the mixture was cooled, water (50 mL) and a solution of 30% sulfuric acid (10 mL) were added. The product was extracted with hexane (150 mL), and the extract was washed with water (3 × 200 mL). The extract was dried over Na_2SO_4, the solvent was removed on a rotary evaporator, and the residue was recrystallized from hexane. 3,6-Di-*tert*-butyl-2-methoxyphenol was isolated as a white finely crystalline powder. The yield was 9.58 g (72%).

For $C_{15}H_{24}O_2$		
Anal. calcd., %	C, 76.23	H, 10.24
Found, %	C, 76.48	H, 10.52

^{1}H NMR ($CDCl_3$; 200 MHz; δ, ppm): 1.42 (s, 9H, *t*-Bu), 1.43 (s, 9H, *t*-Bu), 3.83 (s, 3H, OCH_3), 5.77 (s, 1H, OH), 6.82 (d, 1H, C_{ar}–H, $J = 8.5$ Hz), 6.99 (d, 1H, C_{ar}–H, $J = 8.5$ Hz). ^{13}C NMR ($CDCl_3$; 50 MHz; δ, ppm): 29.53, 31.15, 34.49, 34.73 (C, *t*-Bu); 61.33 (OCH_3), 117.39, 121.57 (C_{ar}–H); 135.06, 140.18, 147.06, 148.56 (C_{ar}).

3,6-Di-tert-butyl-4-(3,6-di-tert-butyl-2-methoxyphenoxy)-2-methoxycyclohexa-2,5-dien-1-one.

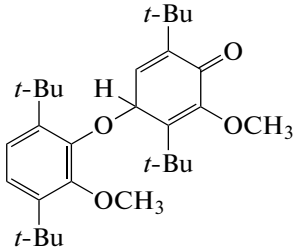

An aqueous solution containing KOH (1.34 g, 0.024 mol) and $K_3Fe(CN)_6$ (11.84 g, 0.036 mol) was added with vigorous stirring to a solution of 3,6-di-*tert*-butyl-2-methoxyphenol (5.54 g, 0.024 mol) in diethyl ether. The reaction mixture was stirred at room temperature for 1 h. Then the product was extracted with ether, washed with water (3 × 100 mL), and dried over sodium sulfate. The solvent was evaporated on a rotary evaporator. The obtained product was recrystallized from hexane. The yield of yellow-green crystals of 3,6-di-*tert*-butyl-4-(3,6-di-*tert*-butyl-2-methoxy-

phenoxy)-2-methoxycyclohexa-2,5-dien-1-one was 1.55 g (28%).

For $C_{30}H_{46}O_4$		
Anal. calcd., %	C, 76.55	H, 9.85
Found, %	C, 76.53	H, 9.81

^{1}H NMR ($CDCl_3$; 200 MHz; δ, ppm): 0.92, 1.24, 1.40, 1.50 (s, 9H, *t*-Bu); 3.75 (s, 3H, OCH_3), 3.88 (s, 3H, OCH_3), 5.94 (d, 1H, C–H, J = 4.6 Hz), 6.45 (d, 1H, C_{ar}–H, J = 4.6 Hz), 6.93 (s, 2H, C_{ar}–H). ^{13}C NMR ($CDCl_3$; 50 MHz; δ, ppm): 28.87, 29.85, 30.42, 30.88 (CH_3, *t*-Bu); 34.42, 34.63, 34.76, 35.64 (C_q, *t*-Bu); 59.39, 61.52 (OCH_3); 69.47 (C–H); 120.69, 121.22, 137.30, 141.13, 141.72, 144.02 (C_{ar}); 147.16, 149.65, 152.53, 152.97 (C); 182.68 (C=O).

Synthesis of complex ^{Phenox}APGe (I). A weighed sample of iminoquinone ^{Phenox}imQ (0.4 g, 0.95 mmol) dissolved in tetrahydrofuran (THF) (5 mL) was added to an excess of finely cut metallic lithium. The reaction was carried out on slight heating with stirring until the color changed from bright blue to yellow. The resulting solution of dilithium salt ^{Phenox}APLi$_2$ was added to germanium dichloride dioxanate (0.219 g, 0.95 mmol). The reaction mixture was held in a water bath for 1 h, and the process was accompanied by the precipitation of lithium chloride and change in color to intensive orange. THF was removed under reduced pressure, and the residue was dissolved in toluene and filtered from a LiCl precipitate using a syringe filter in a glove box under an inert atmosphere. After the solution was concentrated by three times, orange crystalline product **I** was isolated. The yield was 0.379 g (0.75 mmol, 81%).

For $C_{28}H_{41}NO_2Ge$			
Anal. calcd., %	C, 68.04	H, 7.95	N, 2.83
Found, %	C, 68.33	H, 8.14	N, 2.70

^{1}H NMR (C_6D_6; 20°C; δ, ppm): 7.1, 7.09, 6.99 (d, 1H, H_{AP}, $J_{H,H}$ = 2.27 Hz); 1.7 (s, 9H, N(*t*-Bu)); 1.66, 1.62, 1.28 (s, 9H, *t*-Bu). ^{13}C NMR (C_6D_6; 20°C; δ, ppm): 152.3, 144.7 (C_{AP}); 139.3, 138.5, 137.5 (C–O); 131.4, 129.9 (C–N); 126.5, 126.0, 119.5, 116.1, 112.7 (C_{AP}); 35.1, 34.4, 34.2, 34.0 (C_q); 31.06, 30.9, 30.5, 29.4 (CH_3, *t*-Bu).

Synthesis of complex (^{Phenox}APGe)$_4$Ni (II). An equimolar quantity of complex **I** (0.35 g, 0.711 mmol) dissolved in toluene was added to a solution (frozen in liquid nitrogen) of bis(cyclooctadienyl) nickel (0.048 g, 0.17 mmol) in the same solvent (3 mL). Then the reaction mixture was gradually heated to room temperature. The resulting solution was stored for 2 days in the dark to complete the reaction, and the solution turned red-brown during this time. After concentrating, brown finely crystalline complex **II** was isolated from the solution and dried on heating under reduced pressure. The yield was 0.86 g (0.43 mmol, 61%).

For $C_{112}H_{164}N_4O_8NiGe_4$			
Anal. calcd., %	C, 66.08	H, 7.72	N, 2.75
Found, %	C, 66.45	H, 7.96	N, 2.51

^{1}H NMR (C_6D_6; 20°C; δ, ppm): 7.03, 6.94, 6.81 (d, 1H, H_{AP}); 1.58 (d, 18H, *t*-Bu); 1.31, 1.27 (s, 9H, *t*-Bu). ^{13}C NMR (C_6D_6; 20°C; δ, ppm): 145.1 (C_{AP}); 140.3, 138.6, 136.3 (C–O); 130.8, 130.3 (C–N); 129.1, 128.9, 122.7, 116.3, 115.1, 110.8 (C_{AP}); 34.8, 34.4, 33.9, 33.7 (C_q); 31.13, 30.8, 30.6, 29.9 (CH_3, *t*-Bu).

Synthesis of complex (^{Phenox}APGe)$_2$(NiCp)$_2$ (III). A weighed sample of complex **I** (0.35 g, 0.711 mmol) dissolved in toluene was added to a solution of nickel cyclopentadienylcarbonyl dimer (0.215 g, 0.711 mmol) in the same solvent (5 mL). Then the reaction mixture was stored for 2 days in the dark to complete the reaction, and the solution turned brown within this time. Red-brown finely crystalline complex **III** was isolated from a concentrated solution in hexane. The yield was 0.48 g (0.38 mmol, 54%).

For $C_{66}H_{92}N_2O_4Ni_2Ge_2$			
Anal. calcd., %	C, 66.22	H, 7.36	N, 2.09
Found, %	C, 66.51	H, 7.48	N, 2.1

^{1}H NMR (C_6D_6; 20°C; δ, ppm): 7.5, 7.2, 7.0 (d, 1H, H_{AP}, $J_{H,H}$ = 2.02 Hz); 5.15 (s, 5H, Cp); 1.74, 1.69, 1.67, 1.36 (s, 9H, *t*-Bu). ^{13}C NMR (C_6D_6; 20°C; δ, ppm): 151.6, 144.5 (C_{AP}); 139.4, 138.1, 137.7 (C–O); 132.3, 130.06 (C–N); 128.9, 126.7, 118.5, 114.9, 111.3 (C_{AP}); 88.29 (Cp); 37.1, 35.27, 34.71, 34.36 (C_q); 31.19, 31.02, 30.59, 29.6 (CH_3, *t*-Bu).

Synthesis of complex [(^{Phenox}APGe)$_2$O][Im] (VI). A vigorously stirred mixture of toluene (7 mL) and H_2O (0.2 mmol, 3.64 μL) (sampled with a micropipette) was added with a solution of germylene **I** (0.2 g, 0.4 mmol) in the same solvent (10 mL). The reaction mixture gained a yellow tint, was stored for 1 h with vigorous stirring, and then used without isolation. A solution of 1,3-diisopropyl-4,5-dimethylimidazol-2-ylidene (0.4 mmol, 0.072 g) in toluene was poured to the reaction mixture. After the end of the reaction, pale yellow finely crystalline complex **VI** precipitated from the solution. The yield was 0.27 g (50%). Calculated: C, 68.48; H, 8.91; N, 6.14. Found: C, 68.59; H, 9.03; N, 6.25.

^{1}H NMR (C_6D_6; 20°C; δ, ppm): 7.11 (d, 1H, H_{AP}); 6.69 (s, 2H, H_{AP}); 3.8 (m, CH, *i*-Pr); 1.75, 1.72, 1.69, 1.37 (s, 9H, *t*-Bu), 1.35 (s, 6H, C–Me); 1.22 (d, 12H, CH_3, *i*-Pr). ^{13}C NMR (C_6D_6; 20°C; δ, ppm): 145.1

(C_{AP}); 140.3, 138.6, 136.3 (C–O); 130.8, 130.3 (C–N); 129.1, 128.9, 122.7, 116.3, 115.1, 110.8 (C_{AP}); 34.03, 34.0, 34.4, 34.7 (C_q); 31.63, 31.45, 30.9, 30.0 (CH_3, *t*-Bu); 22.06 (CH_3, *i*-Pr); 7.55 (CH_3).

Synthesis of complex [(^{Phenox}APGe)$_2$O][K(THF)$_3$] (VII). The hydrolysis of germylene **I** was carried out similarly to that described above. The solvent was removed under reduced pressure, and the residue was dissolved in THF (10 mL). The resulting solution was poured to KC_8 (0.054 g, 0.4 mmol). The reaction mixture was stored with stirring for 2 days. Colorless crystals of complex **VII** were isolated from the solution after filtration from formed graphite and concentrating. The compound turned out to be very unstable and rapidly decomposed after isolation from the solvent and, hence, no satisfactory analytical data were obtained. The molecular structure was determined by single-crystal X-ray diffraction (XRD).

XRD of compounds **I** and **VII** was carried out on Bruker APEX II and Bruker D8 Venture diffractometers, respectively, at the Center for Collective Use of the Kurnakov Institute of General and Inorganic Chemistry (Russian Academy of Sciences). Primary indexing, unit cell parameter refinement, and reflection integration were performed using the Bruker APEX3 program package [49]. An absorption correction of reflection intensities was applied using the SADABS program [49]. The diffraction data on the crystals of compound **II** were collected on a Rigaku OD Xcalibur E diffractometer. Experimental sets of intensities for compound **II** were integrated using the CrysAlisPro program [50]. An absorption correction was applied using the SCALE3 ABSPACK algorithm [50]. The XRD data for compound **III** were obtained on the X-ray beamline of the Belok station at the Kurchatov Synchrotron Radiation Source of the National Research Center "Kurchatov Institute" (Moscow, Russia) using a Rayonix SX165 CCD detector [51]. Unit cell parameters were determined and refined, reflections were integrated, and an absorption correction of reflection intensities was applied using the XDS program package [52].

The structures were solved by direct methods and refined by full-matrix least squares for F^2 in the anisotropic approximation for all non-hydrogen atoms [53, 54]. Hydrogen atoms were placed in the geometrically calculated positions and refined isotropically with fixed thermal parameters $U(H)_{iso} = 1.2U(C)_{equiv}$ ($U(H)_{iso} = 1.5U(C)_{equiv}$ for methyl groups).

The SIMU, RIGU, DELU, ISOR, EADP, and SADI instructions were applied to the structure refinement of compound **III** in the case of strong disordering. The residual electron density related to the disordered neutral solvent in the structure of compound **III** was removed using the SQUEEZE procedure in the PLATON program [55].

The crystallographic data, XRD experimental parameters, and structure refinement results are presented in Table 1.

The calculations were performed using the SHELXTL software [54] in the OLEX2 medium of structural data visualization and processing [54].

The structures were deposited with the Cambridge Crystallographic Data Centre (CIF files CCDC nos. 2117783 (**I**), 2124277 (**II**), 2125357 (**III**), 2118393 and (**VII**); ccdc.cam.ac.uk/structures).

RESULTS AND DISCUSSION

The germanium(II) *o*-amidophenolate complex ^{Phenox}APGe (**I**) was synthesized using the two-step method. At the first stage, iminoquinone was reduced with an excess of alkaline metal, and the dilithium derivative was used further without isolation. The next stage was the exchange of dilithium salt ^{Phenox}APLi$_2$ with $GeCl_2$·diox (Scheme 1).

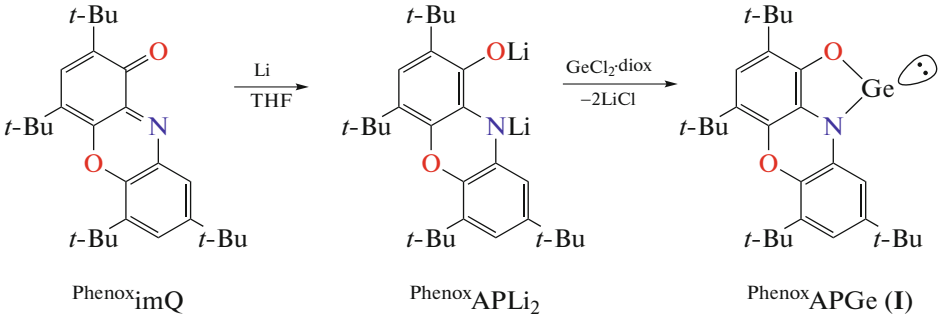

^{Phenox}imQ ^{Phenox}APLi$_2$ ^{Phenox}APGe (**I**)

Scheme 1.

Complex **I** is a bright orange crystalline substance sensitive to air moisture and oxygen and highly soluble in the most part of organic solvents. Single-crystal samples suitable for XRD were obtained from a concentrated solution in toluene. According to the data obtained, compound **I** is a monomeric complex in which one dianionic ligand chelates the low-valent Ge atom via the bidentate mode (Fig. 1). The C–O

Table 1. Crystallographic data and experimental and structure refinement parameters for compounds **I**, **II**, **III**, and **VII**

Parameter	Value			
	I	**II**	**III**	**VII**
Empirical formula	$C_{28}H_{39}NO_2Ge$	$C_{112}H_{156}N_4O_8NiGe_4$, $4C_7H_8$	$C_{73}H_{96}N_2O_4Ni_2Ge_2$	$C_{68}H_{100}N_2O_8K_2Ge_2$
FW	494.19	2404.00	1328.11	1296.87
Crystal system	Orthorhombic	Triclinic	Monoclinic	Orthorhombic
Space group	*Pnma*	$P\bar{1}$	*P*21/*m*	*Pbca*
T, K	150	110	100	100
λ, Å	0.71073 (Mo)	0.71073 (Mo)	0.74500 (synchrotron)	1.54178 (Cu)
a, Å	9.2209(7)	18.1898(3)	19.690(4)	18.4255(5)
b, Å	27.822(2)	18.3046(3)	9.7250(19)	26.6762(7)
c, Å	10.0187(9)	20.5844(4)	19.904(4)	27.8650(8)
α, deg	90	76.862(2)	90	90
β, deg	90	82.252(2)	111.46(3)	90
γ, deg	90	84.212(2)	90	90
V, Å^3	2570.2(4)	6595.9(2)	3547.2(14)	13696.3(6)
Z	4	2	2	8
ρ_{calc}, g/cm^3	1.277	1.210	1.243	1.258
μ, mm^{-1}	1.216	1.096	1.579	2.578
Crystal size, mm	0.30 × 0.30 × 0.28	0.42 × 0.24 × 0.11	0.240 × 0.080 × 0.040	0.11 × 0.05 × 0.02
Scan range over θ, deg	2.93–30.55	2.91–26.02	1.165–26.357	3.31–66.98
Number of measured/ independent reflections	29278/3976	91144/25958	30756/6622	110103/12032
R_{int}	0.0350	0.0775	0.1275	0.0980
Number of independent reflections with $I > 2\sigma(I)$	3337	17217	6622	8776
Number of refined parameters/ restraints	184/0	1640/441	377/575	862/101
R ($F^2 > 2\sigma(F^2)$)	$R_1 = 0.0367$, $wR_2 = 0.0956$	$R_1 = 0.0596$, $wR_2 = 0.1389$	$R_1 = 0.0898$, $wR_2 = 0.2328$	$R_1 = 0.0663$, $wR_2 = 0.1551$
R (for all data)	$R_1 = 0.0453$, $wR_2 = 0.1004$	$R_1 = 0.1049$, $wR_2 = 0.1605$	$R_1 = 0.1478$, $wR_2 = 0.2777$	$R_1 = 0.0938$, $wR_2 = 0.1667$
S (F^2)	1.031	1.036	1.027	1.076
Residual electron density (max/min), e/Å^3	0.45/–0.25	1.48/–0.69	1.436/–1.288	0.54/–0.45

(1.350(2) Å) and C–N (1.401(2) Å) bond lengths in the chelate fragment lie in the range characteristic of the dianionic form of this ligand [32]. The C–C bond lengths in the six-membered cycles lie in a range of 1.391(2)–1.407(2) Å and are typical of aromatic systems. The Ge–N (1.879(2) Å) and Ge–O (1.830(2) Å) distances are slightly longer than similar distances in the known *N*-heterocyclic germylenes [56–60] and alkoxygermylenes [61, 62]. The value of the NGeO angle (86.00(5)°) is characteristic of compounds of this class. The Ge...π_{aryl} interaction (3.25 Å) is observed in the crystal between the adjacent monomeric germylene fragments. Coordination chains are formed in the crystal packing of compound **I** due to this interaction. An important distinction of germylene **I** from similar Sn [12, 13, 63] and Pb [11] *o*-amidophenolate complexes is the absence of Ge...O and Ge...N intermolecular contacts between adjacent fragments.

Like other diimine, catecholate [44, 64, 65], and amidophenolate [11–16, 44, 45] complexes of low-valent group 14 metals, synthesized *o*-amidophenolate complex **I** can demonstrate versatile reactivity. The low-valent metal atom can enter into oxidative addition reactions to form tetravalent derivatives. At the same time, the redox-active ligand can be involved in the redox interaction with the retention of the oxidation state of the metal. Owing to the presence of a lone pair and a vacant *p* orbital, metallenes manifest the Lewis amphoteric character: they can act as both soft acids and soft bases.

There are vast published data on the complex formation of low-valent group 14 element derivatives with transition metals by the involvement of the lone electron pair of metallene into the interaction [66]. It should be mentioned that metallenes act as Lewis bases in this case. The reaction of compound **I** with $Ni(COD)_2$ in a toluene solution completes at room temperature within 2 days and gives adduct **II** as a brown finely crystalline powder (Scheme 2).

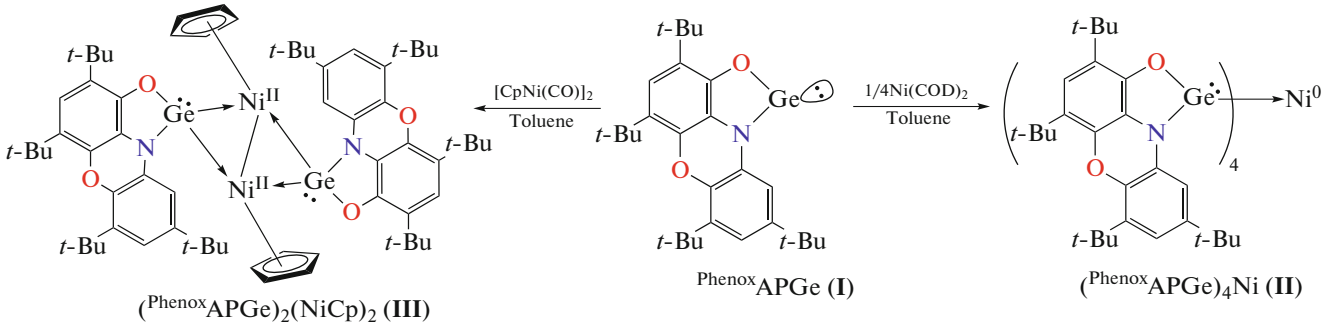

Scheme 2.

According to the XRD data (Fig. 2), complex **II** is a zero-valent nickel compound bound by coordination interactions to four neutral germylenes. The retention of the divalent state of germanium during this reaction is confirmed by the bond length distribution around the metal center. The C–O (1.366(5)–1.380(5) Å) and C–N (1.395(5)–1.406(5) Å) bond lengths in the chelate fragments are comparable with similar characteristics of starting complex **I** (C–O 1.350(2) Å, C–N 1.401(2) Å). The Ge–O and Ge–N (1.830(2) Å, 1.879(2) Å) distances in compound **I** and the average values in compound **II** (1.807 and 1.842 Å, respectively) somewhat shorten in the course of coordination of germylene **I** to nickel. The tetrahedral environment is characteristic of Ni^0 coordinated by four carbene analogs [67–69] and is provided by the donor-acceptor interaction of lone electron pairs of germanium and vacant orbitals of nickel. The Ge–Ni (2.1911(7)–2.2050(7) Å) distances in heterometallic complex **II** are significantly shorter than similar interactions in the previously published tetrasubstituted nickel derivatives [67–69]. This is explained by the decreasing in steric loading of the Ge(II) atom on going from *N*,*N*-heterocyclic germylenes to the *O*,*N*-chelate cycle in derivative **I**.

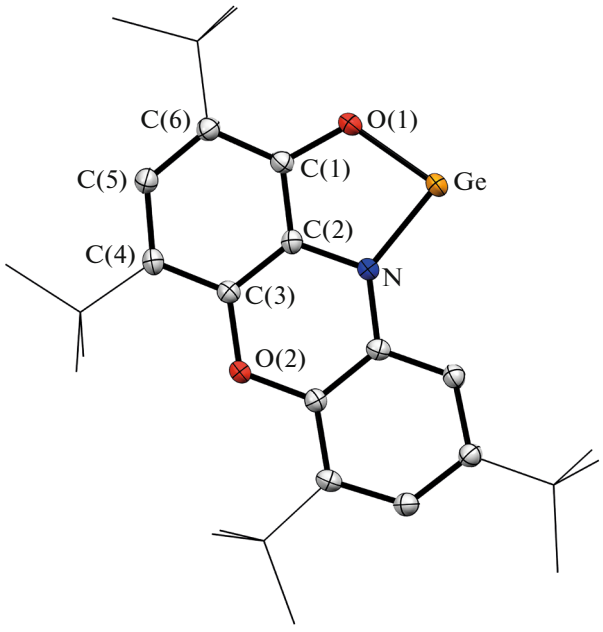

Fig. 1. Molecular structure of complex PhenoxAPGe (**I**). Thermal ellipsoids of selected atoms are given with 50% probability. Hydrogen atoms are omitted for clarity.

The reaction of compound **I** with the dimeric nickel compound $[CpNi(CO)]_2$ in a toluene solution ceases within 2 days at room temperature and is accompanied by CO evolution and a change in the color from red to brown (Scheme 2). Red-brown complex **III** was isolated after the solvent was changed to hexane and the solution was concentrated by approximately three times.

According to the XRD data (Fig. 3), complex **III** is the product of substitution of two carbonyl groups by two isolobal germylene fragments. The unit cell of the crystal contains one molecule of solvated toluene per

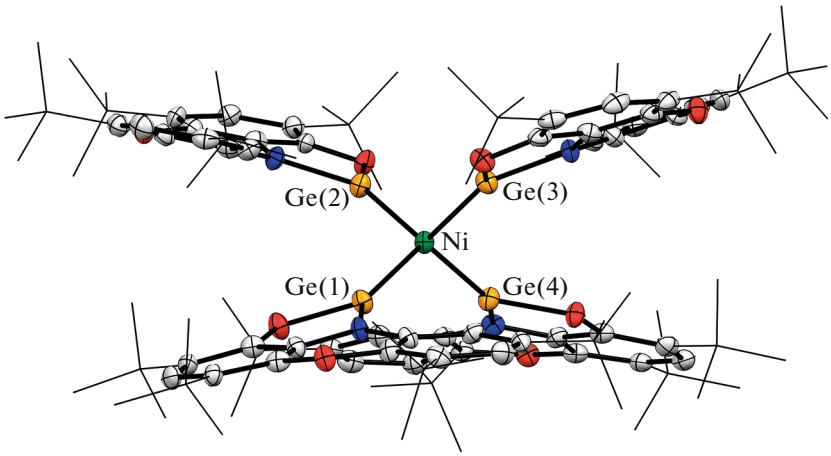

Fig. 2. Molecular structure of complex (^{Phenox}APGe)$_4$Ni (**II**). Thermal ellipsoids of selected atoms are given with 50% probability. Hydrogen atoms are omitted for clarity.

molecule of the complex. The both germylene fragments lie in one plane. A molecule of complex **III** contains the Ge_2Ni_2 core in the "butterfly" configuration with the Ni–Ni bond equal to 2.581 Å, which is somewhat longer than a similar interaction in the starting dimer (2.363 Å) [70]. The Ge···Ge distance is 3.379 Å indicating the absence of an attractive interaction between the atoms. The dihedral angle between the Ni–Ge(1)–Ni and Ni–Ge(2)–Ni planes forming "butterfly wings" is 135.8°, which is smaller than a similar angle in $[CpNi(CO)]_2$. Both Ni atoms are arranged at equal distances of 1.730 Å from the centroids of their Cp ligands. Both cyclopentadienyl ligands are nonsymmetrically coordinated to their nickel atoms via the pseudo-π-allyl mode. These distortions are usually caused by the nonequivalence of the monodentate *trans*-ligands in the half-sandwich complexes [71]. The donor-acceptor Ge–Ni interactions in complex **III** range from 2.223 to 2.244 Å, which satisfactorily corresponds to those in complex **II**. The Ge–O and Ge–N distances (average values in **III** are 1.792 and 1.874 Å, respectively) shorten during coordination compared to those in germylene **I** and resemble those in compound **II**. The C–O (1.256(15)–1.304(15) Å) and C–N (1.378(14)–1.408(15) Å) bonds in the chelate fragments are slightly shorter than analogous characteristics of compounds **I** and **II** but lie in the range characteristic of the dianionic structure of the amidophenolate ligands [32]. A solution of complex **III** is diamagnetic, exhibits a well resolved NMR spectrum, and has no signals in the EPR spectrum. This confirms that nickel and germanium retain their oxidation states during the reaction (Scheme 2).

Heterometallic complex **III** is the second example of the stabilization of the CpNi–NiCp fragment in the coordination compound with germylenes. Complex $[(C_6F_5)_2GeNiCp]_2$ synthesized by the redox reaction of tetrakis(pentafluorophenyl)dihydrodigermane and nickelocene is the single presently known compound containing the cluster with the similar structure [72]. The intermediate formation of germylene $(C_6F_5)_2Ge$, which coordinates to the nickel atom upon generation in the reaction mixture, was proposed [72]. The structure of the central fragment of the previously published complex $[(C_6F_5)_2GeNiCp]_2$ is nearly identical to that of complex **III** except for a considerably smaller dihedral angle between the "butterfly wings" (117.6 Å).

Metallenes similar to germylene **I** possess two possible reducing centers: (a) the low-valent germanium atom that can participate in oxidative addition followed by the formation of the germanium(IV) derivatives and (b) the redox-active *o*-amidophenolate ligand that can undergo redox processes without changing the oxidation state of tetrylene. The both centers are reactive and can individually be activated depending on the oxidant nature [11–15, 44, 45, 73]. It is known that the tetrylene derivatives with various dianionic redox-active ligands (diamide, amidophenolate, catecholate) react with stable radicals or Hg(II) and Ag(I) halides to form the corresponding radical compounds ranging from those detected by EPR spectroscopy only [64, 65, 74–76] to stable compounds [77, 78]. As a rule, these paramagnetic derivatives of heavy carbene analogs can be observed for tin(II) and lead(II) compounds. However, in the case of germanium(II), the low-valent center is predominantly oxidized and, hence, the participation of the *o*-amidophenolate ligands in the oxidation of *O*,*N*-heterocyclic germylenes was not observed earlier [14, 15]. Nevertheless, the first example of paramagnetic germylene based on sterically hindered *N*-adamantyl-3,5-di-*tert*-butyl-*o*-aminophenol has recently been reported [16]. This compound was detected in the reaction mixture by EPR spectroscopy, but a low sta-

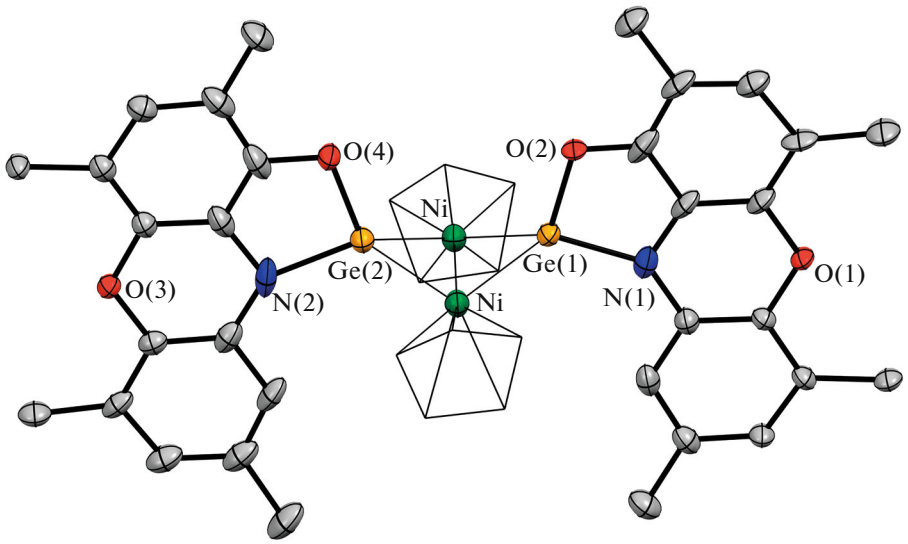

Fig. 3. Molecular structure of complex (^{Phenox}APGe)$_2$(NiCp)$_2$ (**III**). Thermal ellipsoids of selected atoms are given with 30% probability. Hydrogen atoms and *tert*-butyl groups are omitted for clarity.

bility of the generated compound did not allow one to accumulate the concentration sufficient for the observation of the hyperfine coupling (HFC) of the unpaired electron with the magnetic ^{73}Ge isotope.

We performed the chemical oxidation of germylene **I** by the stable 3,6-di-*tert*-butyl-2-methoxyphenoxy radical [48] (Scheme 3). The formation of the paramagnetic heavy analog of carbene (**IV**) was successfully detected by EPR spectroscopy (Fig. 4). The generated compound can be observed in the solution at room temperature within 15–20 min, and after this time the spectrum is supplemented by the whole set of additional signals indicating the further transformation of compound **IV** in the solution.

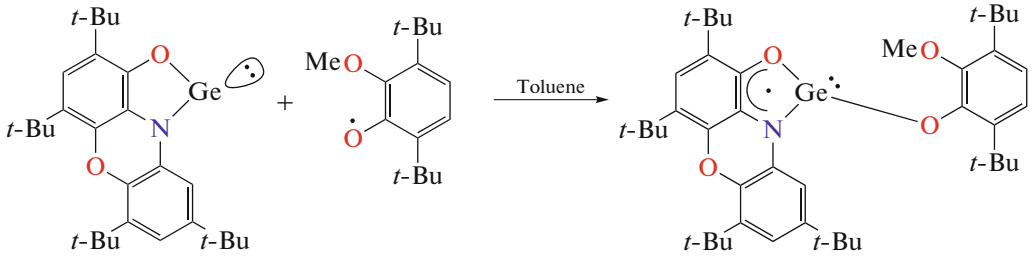

^{Phenox}APGe (**I**) (**IV**)

Scheme 3.

The EPR spectrum of compound **IV** at $T = 300$ K is highly resolved due to a small width (0.3 G) of the individual components of the spectrum. Their hyperfine structure is caused by the HFC of the unpaired electron with magnetic nuclei of three protons ^{1}H (99.98%, $I = 1/2$, $m_N = 2.7928$) and one nitrogen atom ^{14}N (99.63%, $I = 1$, $m_N = 0.4037$). We succeeded to observe the satellite splitting on the ^{73}Ge magnetic isotope (7.8%, $I = 9/2$, $m_N = 0.8795$) at the edges of the main spectrum. The parameters of the spectrum are the following: $g_i = 2.0030$, $a_i(^{14}N) = 8.04$ G; $a_i(^{1}H) = 4.16, 3.18, 2.02$ G; and $a_i(^{73}Ge) = 5.65$ G. It should be mentioned that the HFC constant with the ^{73}Ge magnetic isotope in compound **IV** is almost two times lower compared to the related paramagnetic *N*,*N*-heterocyclic germylenes [75–77]. At the same time, the HFC constant more than 5 times exceeds the values characteristic of the germanium(IV) derivatives with the radical-anion ligands [78]. This fact unambiguously indicates the retention of the divalent state of the germanium atom in the observed paramagnetic compound **IV**. The reasons for such a significant change in the HFC constants in the paramagnetic compounds of group 14 elements in oxidation states of 2 and 4 were discussed in detail [79].

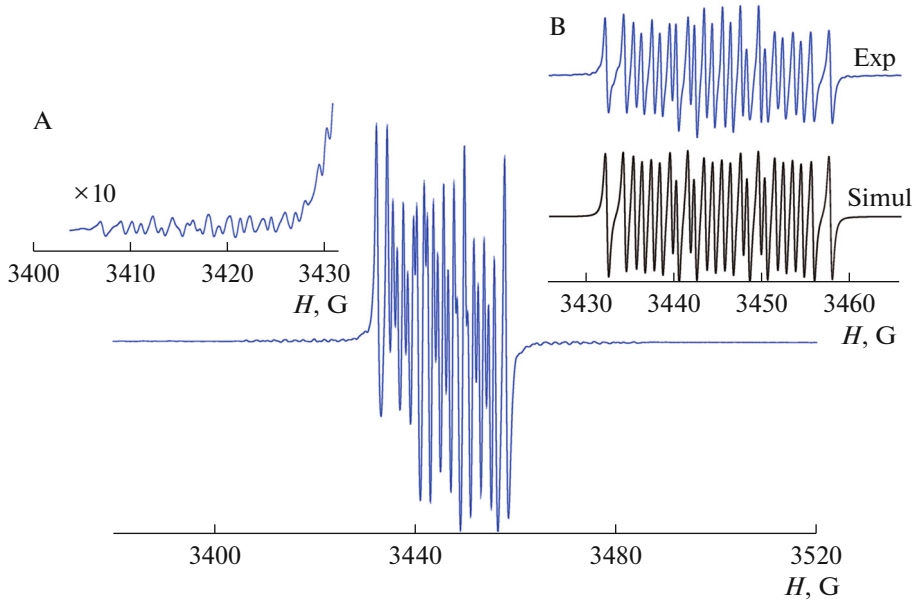

Fig. 4. EPR spectrum of paramagnetic compound **IV** in toluene at $T = 300$ K. Inset A (magnified by 10 times): the range demonstrating the HFC with the ^{73}Ge isotope; inset B (experimental and simulated): central part of the spectrum.

It was shown in the recent studies [80, 81] that the hydrolysis of Ge(II) *o*-amidophenolates led to the formation of the corresponding oxide derivatives in which the germanium(II) atoms can exhibit the stronger nucleophilic properties than those of the starting two-coordinated germylenes. We synthesized digermylene oxide **V** by the reaction of compound **I** with water taken in stoichiometric amounts (Scheme 4). The reaction occurs without additional heating and with vigorous stirring for 1 h. The prolonged crystallization of the reaction mixture leads to the decomposition of complex **V**: the slow evaporation of the solvent after the end of the reaction results in an oily residue, which contains the decomposition products along with target digermylene oxide **V**, in particular, the corresponding *o*-aminophenol. Therefore, we attempted to stabilize the derivative obtained *in situ* by the deprotonation of the *o*-aminophenolate fragments.

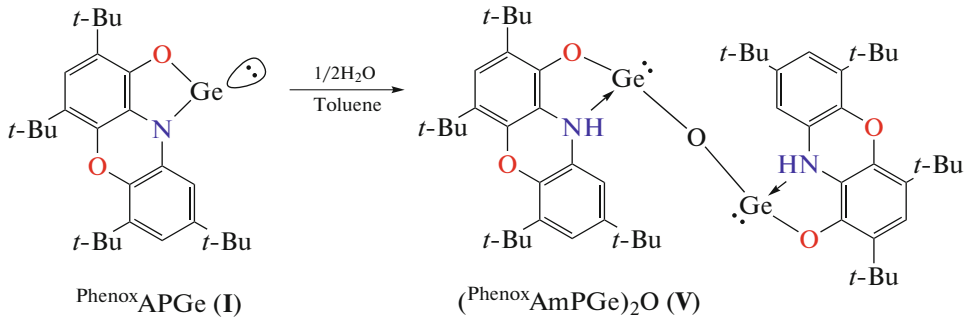

^{Phenox}APGe (**I**) (^{Phenox}AmPGe)$_2$O (**V**)

Scheme 4.

After the hydrolysis of germylene **I**, the treatment of the reaction mixture with *N*,*N*-heterocyclic carbene affords stable ionic complex **VI** (Scheme 5). The reaction occurs with the rate of mixing reactants and ceases when a pale yellow finely crystalline powder spontaneously precipitated (in a high yield). The structure of complex **VI** was confirmed by NMR spectroscopy. We failed to obtain crystals suitable for XRD, but by analogy to the published results [81] we may assert that compound **VI** contains the dianion in which two tricoordinated Ge(II) atoms are linked by bridging oxygen. Two imidazolinium cations act as counterions.

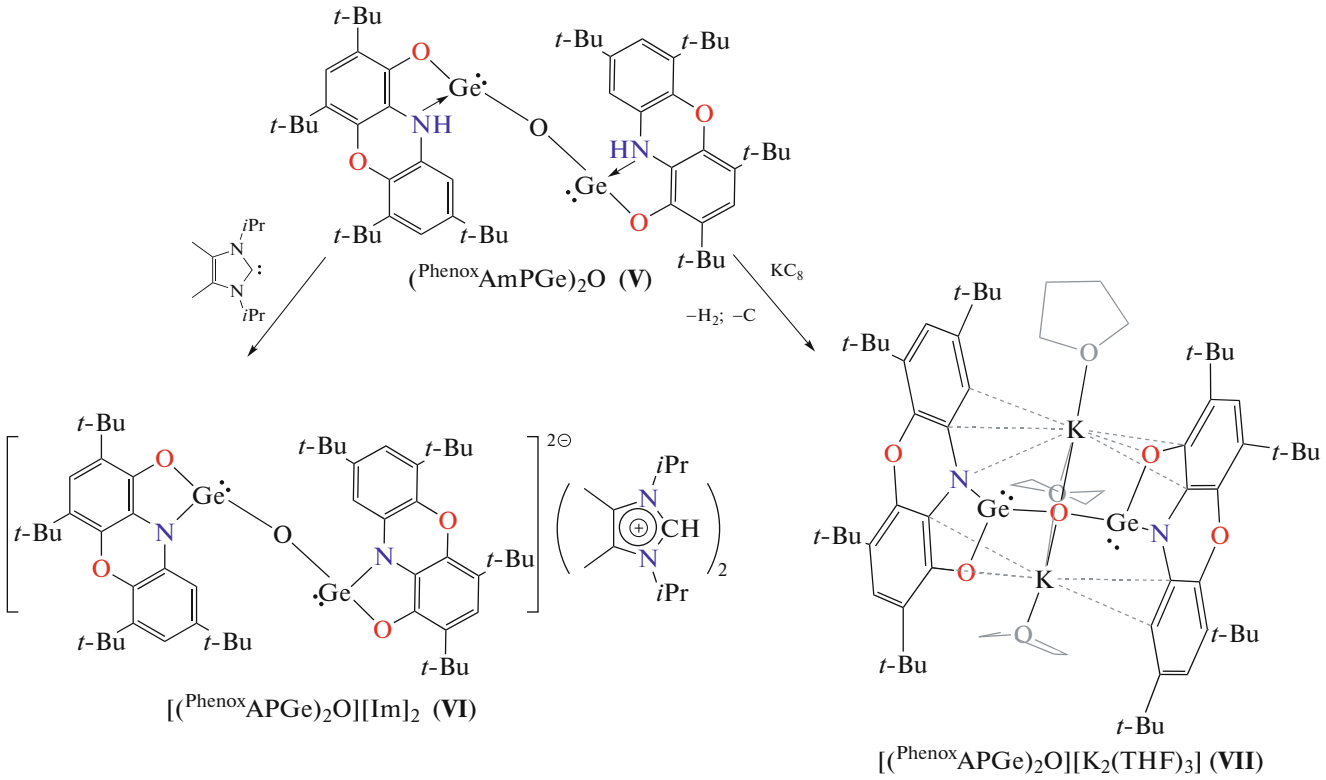

Scheme 5.

The reaction of compound **V** with potassium intercalated in graphite results in the evolution of gaseous hydrogen and formation of compound **VII** isolated in a low yield from the reaction mixture as colorless crystals (Scheme 5). Unlike compound **VI**, complex **VII** is very sensitive to trace amounts of air moisture and oxygen and decomposes upon the removal of the mother liquor. All attempts to detect the NMR spectra of this compound were unsuccessful. The repeated dissolution of the crystalline powder of complex **VII** in deuterated solvents induces its decomposition.

However, we were able to determine the molecular structure of compound **VII** using XRD (Fig. 5). According to the data obtained, the $[(^{Phenox}APGe)_2O]^{2-}$ dianion in compound **VII** is coordinated by two potassium cations, which are solvated, in turn, by three THF molecules. Germanium retains the divalent state. The dianionic fragment in compound **VII** contains two tricoordinated germylene centers linked to each other by the μ^2-oxygen bridge. The GeO(1)Ge angle is 126.3(2)° and much smaller than those in numerous known related tricoordinated germylene derivatives [82, 83]. The Ge–O(1) distances are 1.863(2), 1.867(2) Å and also exceed the values for similar derivatives [83–86]. The sums of angles around the Ge(1) (270.8°) and Ge(2) (268.9°) atoms are close to 270° and indicate a low degree of involving of the lone electron pair localized on the *s* orbital into hybridization. The bond length distribution in the *o*-amidophenolate fragment is typical of similar types of ligands. The Ge–O (1.913(5), 1.920(5) Å) and Ge–N (1.994(4), 1.996(6) Å) distances in compound **VII** are noticeably longer than those in compound **I** (Ge–O 1.830(2) Å, Ge–N 1.879(2) Å). Selected bond lengths for compounds **I**–**III** and **VII** are given in Table 2.

There are numerous examples of using heterocyclic compounds of group 14 low-valent elements as catalysts for the polymerization of lactides and cyanosilylation or hydroboration of carbonyl compounds [85–89]. Hydroboration is the most important reaction of element–boron bond formation in organic chemistry, which is also used for the synthesis of boronate ethers representing the class of most important organic reagents in synthetic chemistry. Organoboron compounds are considered to be stable, simple in handling, and universal reagents for cross-coupling processes. The hydroboration of unsaturated bonds is a direct and efficient route to organoboron compounds [90–93]. The hydroboration catalyzed by Sn and Ge turned out to be a selective route to valuable alkyl boronate ethers and attracts attention of researchers [16, 94–96].

In the framework of this study, germylene **I** was tested as a catalyst of the hydroboration of benzaldehyde by pinacolborane (HBpin) (Scheme 6). In blank experiments, benzaldehyde reacted with one equivalent of HBpin without catalyst at room temperature, and conversion was observed only at the trace level. Compound **I** successfully catalyzes the hydroboration

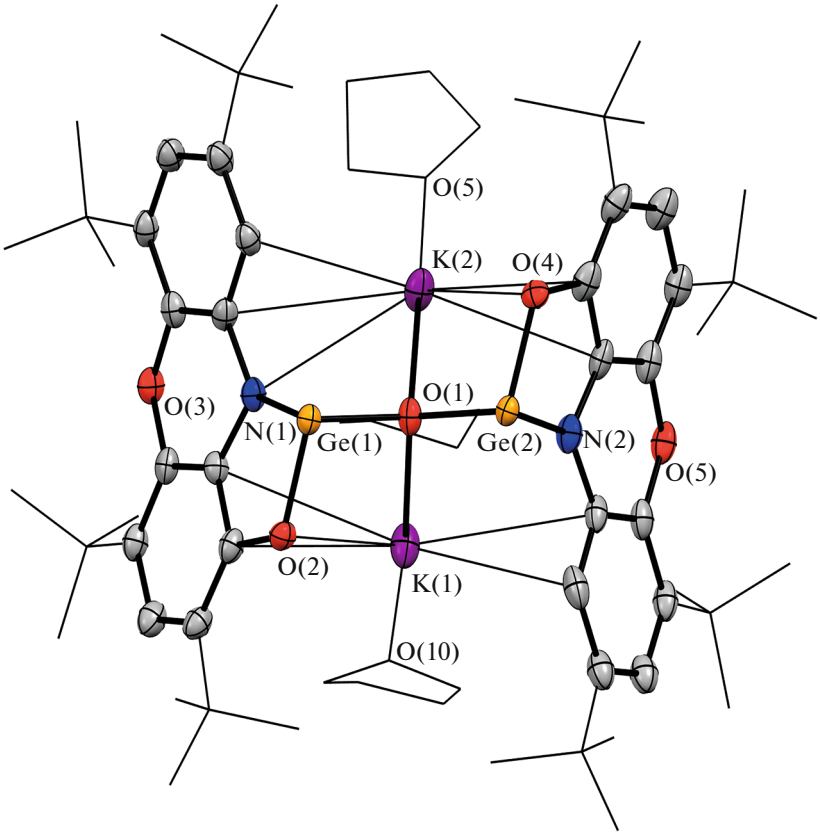

Fig. 5. Molecular structure of complex [(^{Phenox}APGe)$_2$O][K$_2$(THF)$_3$] (**VII**). Thermal ellipsoids of selected atoms are given with 30% probability. Hydrogen atoms are omitted for clarity.

of benzaldehyde with HBpin at room temperature to form the corresponding boronate ether (Scheme 6) with a high conversion within the control time interval. The reaction conditions were optimized and controlled using NMR spectroscopy. The conversions were calculated from the surface area of integration of the product and starting material in the ^{1}H NMR spectra using mesitylene as the internal standard. The results were generalized in Table 3. It is found from the results of the catalytic tests that the activity of germylene **I** as the catalyst of the reaction (Scheme 6) is somewhat lower than that of its closest *O*,*N*-heterocyclic analog based on *N*-adamantyl-3,5-di-*tert*-butyl-*o*-aminophenol [16].

Table 2. Selected bond lengths for complexes **I**, **II**, **III**, and **VII**

Bond (Å)	Complex			
	I	**II**	**III**	**VII**
Ge–N	1.8297(16)	⟨1.842⟩	1.854(8), 1.894(9)	1.994(4), 1.996(6)
Ge–O	1.8785(13)	⟨1.807⟩	1.782(10), 1.802(11)	1.913(5), 1.920(5)
C(1)–O	1.3501(19)	1.366(5)–1.380(5)	1.304(15), 1.256(15)	1.368(5), 1.396(6)
C(2)–N	1.4011(12)	1.395(5)–1.406(5)	1.378(14), 1.408(15)	1.391(6), 1.384(6)
Ge–Ni		2.1911(7)–2.2050(7)	2.2233(17)–2.2440(17)	
Ge–O(1)				1.863(2), 1.867(2)
Ni–Ni			2.581	

Table 3. Conversion (%) of aldehyde in hydroboration catalyzed by germylene **I**

Load of catalyst **I**		1 mol %
substrate	time, h	conversion, %
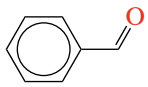	1	61
	2	73
	3	85
	24	91

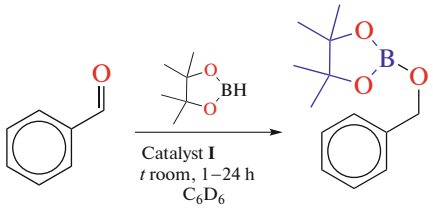

Scheme 6.

Thus, new *O*,*N*-heterocyclic germylene based on redox-active 2,4,6,8-tetra-*tert*-butylphenoxazin-1-one was synthesized and structurally characterized. The synthesized compound can act as a neutral donor ligand due to the lone electron pair of the low-valent germanium atom and can form complexes with both zero-valent and divalent nickel. The oxidation of germanium(II) *o*-amidophenolate by stable radicals affords the paramagnetic heavy analog of carbene that was successfully detected by EPR spectroscopy. The hydrolysis of germylene is accompanied by the formation of the digermylene oxide derivative that can be deprotonated by *N*-heterocyclic carbene or potassium intercalated in graphite. The starting germylene demonstrates catalytic activity in the hydroboration of aldehydes.

ACKNOWLEDGMENTS

This work was carried out using the equipment of the Center for Collective Use "Analytical Center of the Razuvaev Institute of Organometallic Chemistry of the Russian Academy of Sciences" supported by the grant "Provision of Development of Material Technical Infrastructure of Centers for Collective Use of Scientific Equipment" (unique identifier RF–2296.61321X0017, agreement no. 075-15-2021-670).

FUNDING

This work was supported by the Russian Science Foundation, project no. 17-13-01428p.

CONFLICT OF INTEREST

The authors declare that they have no conflicts of interest.

REFERENCES

1. Roesky, P.W., *Dalton Trans.*, 2009, vol. 11, p. 1887.
2. Ochiai, T., Franz, D., and Inoue, S., *Chem. Soc. Rev.*, 2016, vol. 45, p. 6327.
3. Jambor, R. and Dostal, L., *Organometallic Pincer Chemistry. Topics in Organometallic Chemistry*, Koten, G. and Milstein, D., Eds., Berlin: Springer, 2013, vol. 40, p. 175.
4. Yadav, S., Saha, S., and Sen, S.S., *ChemCatChem*, 2015, vol. 8, p. 486.
5. Gendy, C., Rautiainen, M.J., Mailman, A., and Tuononen, H.M., *Chem.-Eur. J.*, 2021, vol. 27, p. 14405.
6. Inoue, S. and Weetman, C., *ChemCatChem*, 2018, vol. 10, p. 4213.
7. Sen, N. and Khan, S., *Chem. Asian. J.*, 2021, vol. 16, p. 705.
8. Zhang, R., Wang, Y., Zhao, Y., et al., *Dalton Trans.*, 2021, vol. 50, p. 13634.
9. Majoumo-Mbe, F., Lönnecke, P., and Hey-Hawkins, E., *Organometallics*, 2005, vol. 24, p. 5287.
10. Ma, M., Shen, L., Wang, H., et al., *Organometallics*, 2020, vol. 39, p. 1440.
11. Tsys, K.V., Chegerev, M.G., Piskunov, A.V., and Fukin, G.K., *Mendeleev Commun.*, 2018, vol. 28, p. 527.
12. Chegerev, M.G., Piskunov, A.V., Tsys, K.V., et al., *Eur. J. Inorg. Chem.*, 2019, p. 875.
13. Piskunov, A.V., Tsys, K.V., Cherkasov, A.V., and Chegerev, M.G., *Russ. J. Coord. Chem.*, 2019, vol. 45, no. 9, p. 626. https://doi.org/10.1134/S1070328419090069
14. Tsys, K.V., Chegerev, M.G., Fukin, G.K., et al., *Mendeleev Commun.*, 2020, vol. 30, p. 205.
15. Arsenyeva, K.V., Ershova, I.V., Chegerev, M.G., et al., *J. Organomet. Chem.*, 2020, vol. 927, p. 121524.
16. Arsenyeva, K.V., Pashanova, K.I., Trofimova, O.Yu., et al., *New J. Chem.*, 2021, vol. 45, p. 11758.
17. Poddel'sky, A.I., Cherkasov, V.K., and Abakumov, G.A., *Coord. Chem. Rev.*, 2009, vol. 253, p. 291.
18. Kaim, W., *Inorg. Chem.*, 2011, vol. 50, p. 9752.
19. Starikova, A.A. and Minkin, V.I., *Usp. Khim.*, 2018, vol. 87, p. 1049.
20. Fomenko, I.S. and Gushchin, A.L., *Usp. Khim.*, 2020, vol. 89, p. 966.
21. Dei, A., Gatteschi, D., Sangregorio, C., and Sorace, L., *Acc. Chem. Res.*, 2004, vol. 37, p. 827.
22. Markevtsev, I.N., Monakhov, M.P., Platonov, V.V., et al., *J. Magn. Magn. Mater.*, 2006, vol. 300, p. e407.
23. Sato, O., *J. Photochem. Photobiol.*, 2004, vol. 5, p. 203.
24. Abakumov, G.A., Cherkasov, V.K., Nevodchikov, V.I., et al., *Inorg. Chem.*, 2001, vol. 40, p. 2434.
25. Pierpont, C.G., *Coord. Chem. Rev.*, 2001, vols. 216/217, p. 99.
26. Meshcheryakova, I.N., Arsenyeva, K.V., Fukin, G.K., et al., *Mendeleev Commun.*, 2020, vol. 30, p. 592.
27. Bubnov, M.P., Kozhanov, K.A., Skorodumova, N.A., et al., *J. Mol. Struct.*, 2019, vol. 1180, p. 87.

28. Kozhanov, K.A., Bubnov, M.P., Teplova, I.A., et al., *J. Mol. Struct.*, 2017, vol. 1147, p. 541.
29. Kozhanov, K.A., Bubnov, M.P., Abakumov, G.A., and Cherkasov, V.K., *J. Magn. Reson.*, 2012, vol. 225, p. 62.
30. Bubnov, M.P., Teplova, I.A., Kozhanov, K.A., et al., *J. Magn. Reson.*, 2011, vol. 209, p. 149.
31. Ivakhnenko, E.P., Karsanov, I.V., Khandkarova, V.S., et al., *Izv. Akad. Nauk SSSR. Ser. Khim.*, 1986, p. 2755.
32. Chegerev, M.G., Arsenyeva, K.V., Cherkasov, A.V., et al., *Russ. J. Coord. Chem.*, 2020, vol. 46, p. 746. https://doi.org/10.1134/S1070328420110019
33. Ivakhnenko, E.P., Koshchienko, Yu.V., Chernyshev, A.V., et al., *Russ. J. Gen. Chem.*, 2016, vol. 86, no. 7, p. 1664.
34. Ivakhnenko, E.P., Koshchienko, Yu.V., Knyazev, P.A., et al., *Russ. J. Coord. Chem*, 2016, vol. 42, p. 509. https://doi.org/10.1134/S1070328416040011
35. Romanenko, G.V., Ivakhnenko, E.P., Minkin, V.I., et al., *Inorg. Chim. Acta*, 2014, vol. 417, p. 66.
36. Ivakhnenko, E.P., Starikov, A.G., Lyssenko, K.A., et al., *Inorg. Chim. Acta*, 2014, vol. 410, p. 144.
37. Antipin, M.Yu., Ivakhnenko, E.P., Koshchienko, Yu.V., et al., *Izv. Akad. Nauk, Ser. Khim.*, 2013, p. 1744.
38. Speier, G., Whalen, A.M., Csihony, J., and Pierpont, C.G., *Inorg. Chem.*, 1995, vol. 34, p. 1355.
39. Bhattacharya, S. and Pierpont, C.G., *Inorg. Chem.*, 1994, vol. 33, p. 6038.
40. Bhattacharya, S. and Pierpont, C.G., *Inorg. Chem.*, 1992, vol. 31, p. 2020.
41. Bhattacharya, S., Boone, S.R., and Pierpont, C.G., *J. Am. Chem. Soc.*, 1990, vol. 112, p. 4561.
42. Ivakhnenko, E.P., Koshchienko, Yu.V., Knyazev, P.A., et al., *Dokl. Ross. Akad. Nauk*, 2011, vol. 438, p. 485.
43. DeLearie, L.A., Haltiwanger, R.C., and Pierpont, C.G., *Inorg. Chem.*, 1989, vol. 28, p. 644.
44. Tsys, K.V., Chegerev, M.G., Pashanova, K.I., et al., *Inorg. Chim. Acta*, 2019, vol. 490, p. 220.
45. Aysin, R.R., Bukalov, S.S., Leites, L.A., et al., *Organometallics*, 2019, vol. 38, p. 3174.
46. Gordon, A. and Ford, R., *The Chemist's Companion: A Handbook of Practical Data, Techniques, and References*, New York: Wiley, 1972.
47. Ryan, S.J., Schimler, S.D., Bland, D.C., and Sanford, M.S., *Org. Lett.*, 2015, vol. 17, p. 1866.
48. Abakumov, G.A., Cherkasov, V.K., Nevodchikov, V.I., et al., *Tetrahedron Lett.*, 2005, vol. 46, p. 4095.
49. *APEX3, SAINT and SADABS*, Madison: Bruker AXS Inc., 2016.
50. *Rigaku Oxford Diffraction. CrysAlisPro Software System. Version 1.171.38.46*, Wroclaw: Rigaku Corporation, 2015.
51. Svetogorov, R.D., Dorovatovskii, P.V., and Lazarenko, V.A., *Cryst. Res. Tech.*, 2020, vol. 55, p. 1900184.
52. Kabsch, W., *Acta Crystallogr., Sect. D: Biol. Crystallogr.*, 2010, vol. 66, p. 125.
53. Sheldrick, G.M., *Acta Crystallogr., Sect. A: Found. Adv.*, 2015, vol. 71, p. 3.
54. Sheldrick, G.M., *Acta Crystallogr., Sect. C*: *Struct. Chem.*, 2015, vol. 71, p. 3.
55. Spek, A.L., *Acta Crystallogr., Sect. C*: *Struct. Chem.*, 2015, vol. 71, p. 9.
56. Matson, E.M., Opperwall, S.R., Fanwick, P.E., and Bart, S.C., *Inorg. Chem.*, 2013, vol. 52, p. 7295.
57. Chegerev, M.G., Piskunov, A.V., Starikova, A.A., et al., *Eur. J. Inorg. Chem.*, 2018, p. 1087.
58. Hill, M.S., *Science*, 2006, vol. 311, p. 1904.
59. Aysin, R.R., Leites, L.A., Bukalov, S.S., et al., *Inorg. Chem.*, 2016, vol. 55, p. 4698.
60. Zabula, A.V., Hahn, F.E., Pape, T., and Hepp, A., *Organometallics*, 2007, vol. 26, p. 1972.
61. Zemlyansky, N.N., Borisova, I.V., Khrustalev, V.N., et al., *Organometallics*, 2003, vol. 22, p. 5441.
62. Kitschke, P., Mertens, L., Rüffer, T., et al., *Eur. J. Inorg. Chem.*, 2015, p. 4996.
63. Aivaz'yan, I.A., Piskunov, A.V., Fukin, G.K., et al., *Inorg. Chem. Commun.*, 2006, vol. 9, p. 612.
64. Chegerev, M.G., Piskunov, A.V., Maleeva, A.V., et al., *Eur. J. Inorg. Chem.*, 2016, p. 3813.
65. Piskunov, A.V., Aivaz'yan, I.A., Cherkasov, V.K., and Abakumov, G.A., *J. Organomet. Chem.*, 2006, vol. 691, p. 1531.
66. Baumgartner, J. and Marschner, C., *Rev. Inorg. Chem.*, 2014, vol. 34, p. 119.
67. Gendy, C., Mansikkamäki, A., Valjus, J., et al., *Angew. Chem., Int. Ed. Engl.*, 2019, vol. 58, p. 154.
68. Ullah, F., Kuhl, O., Bajor, G., et al., *Eur. J. Inorg. Chem.*, 2009, vol. 2, p. 221.
69. Bazinet, P., Yap, G.P.A., and Richeson, D.S., *J. Am. Chem. Soc.*, 2001, vol. 123, p. 11162.
70. Byers, L.R. and Dahl, L.F., *Inorg. Chem.*, 1980, vol. 19, p. 680.
71. Hermann, W.A., Herdtcheck, E., Floel, M., et al., *Polyhedron*, 1987, vol. 6, p. 1165.
72. Pankratov, L.V., Nevodchikov, V.I., Zakharov, L.N., et al., *J. Organomet. Chem.*, 1992, vol. 429, p. 13.
73. Piskunov, A.V., Aivaz'ya, I.A., Poddel'sky, A.I., et al., *Eur. J. Inorg. Chem.*, 2008, p. 1435.
74. Tumanskii, B., Pine, P., Apeloig, Y., et al., *J. Am. Chem. Soc.*, 2004, vol. 126, p. 7786.
75. Tumanskii, B., Pine, P., and Apeloig, Y., *J. Am. Chem. Soc.*, 2005, vol. 127, p. 8248.
76. Abakumov, G.A., Cherkasov, V.K., Piskunov, A.V., et al., *Dokl. Ross. Akad. Nauk*, 2005, vol 404, p. 496.
77. Fedushkin, I.L., Khvoinova, N.M., and Baurin, A.Y., *Inorg. Chem.*, 2004, vol. 43, p. 7807.
78. Abakumov, G.A., Cherkasov, V.K., Ermolaev, N.I., et al., *Izv. Akad. Nauk, Ser. Khim.*, 1995, p. 1568.
79. Abakumov, G.A., Cherkasov, V.K., Piskunov, A.V., et al., *Izv. Akad. Nauk, Ser. Khim.*, 2006, p. 1103.
80. Janes, T., Zatsepin, P., and Song, D.T., *Chem. Commun.*, 2017, vol. 53, p. 3090.
81. Arsenyeva, K.V., Chegerev, M.G., Cherkasov, A.V., et al., *Mendeleev Commun.*, 2021, vol. 31, p. 330.
82. Piskunov, A.V., Arsenyeva, K.V., Klimashevskaya, A.V., and Cherkasov, A.V., *Russ. J. Coord. Chem.,* 2022, vol. 48, p. 278. https://doi.org/10.1134/S1070328422050074
83. Siwatch, R.K., Yadav, D., Mukherjee, G., et al., *Inorg. Chem.*, 2013, vol. 52, p. 13384.

84. Hadlington, T.J., Kefalidis, C.E., Maron, L., and Jones, C., *ACS Catal.*, 2017, vol. 7, p. 1853.
85. Kelly, J.A., Juckel, M., Hadlington, T.J., et al., *Chem.-Eur. J.*, 2019, vol. 25, p. 2773.
86. Pal, S., Dasgupta, R., and Khan, S., *Organometallics*, 2016, vol. 35, p. 3635.
87. Rittinghaus, R.D., Tremmel, J., Růžička, A., et al., *Chem.-Eur. J.*, 2020, vol. 26, p. 212.
88. Praban, S., Yimthachote, S., Kiriratnikom, J., et al., *J. Polym. Sci., Part A*, 2019, vol. 57, p. 2104.
89. Karmakar, A., Hazra, S., Rubio, G.M.D.M., et al., *New J. Chem.*, 2018, vol. 42, p. 17513.
90. Goswami, B., Feuerstein, T.J., Yadav, R., et al., *Chem.-Eur. J.*, 2021, vol. 27, p. 4401.
91. Yadav, S., Dixit, R., Bisai, M.K., et al., *Organometallics*, 2018, vol. 37, p. 4576.
92. Eedugurala, N., Wang, Z., Chaudhary, U., et al., *ACS Catal.*, 2015, vol. 5, p. 7399.
93. Garhwal, S., Kroeger, A.A., Thenarukandiyil, R., et al., *Inorg Chem.*, 2021, vol. 60, p. 494.
94. Dasgupta, R., Das, S., Hiwase, S., et al., *Organometallics*, 2019, vol. 38, p. 1429.
95. Dasgupta, R. and Khan, S., *Adv. Organomet. Chem.*, 2020, vol. 74, p. 105.
96. Schneider, J., Sindlinger, C.P., Freitag, S.M., et al., *Angew. Chem., Int. Ed. Engl.*, 2017, vol. 56, p. 333.

Translated by E. Yablonskaya